Connexin 50 and AQP0 are Essential in Maintaining Organization and Integrity of Lens Fibers

Sumin Gu,[1] Sondip Biswas,[2] Luis Rodriguez,[1] Zhen Li,[1] Yuting Li,[1] Manuel A. Riquelme,[1] Wen Shi,[1,3] Ke Wang,[1] Thomas W. White,[4] Matthew Reilly,[5] Woo-Kuen Lo,[2] and Jean X. Jiang[1]

[1]Department of Biochemistry and Structural Biology, University of Texas Health Science Center, San Antonio, Texas, United States
[2]Department of Neurobiology, Morehouse School of Medicine, Atlanta, Georgia, United States
[3]The Second Xiangya Hospital, Central South University, Changsha, China
[4]Department of Physiology and Biophysics, Stony Brook University, Stony Brook, New York, United States
[5]Department of Biomedical Engineering, The Ohio State University College of Engineering, Columbus, Ohio, United States

Correspondence: Jean X. Jiang, Department of Biochemistry and Structural Biology, University of Texas Health Science Center, 7703 Floyd Curl Drive, San Antonio, TX 78229-3900, USA;
jiangj@uthscsa.edu.

Submitted: November 26, 2018
Accepted: August 19, 2019

Citation: Gu S, Biswas S, Rodriguez L, et al. Connexin 50 and AQP0 are essential in maintaining organization and integrity of lens fibers. *Invest Ophthalmol Vis Sci*. 2019;60:4021–4032. https://doi.org/10.1167/iovs.18-26270

Purpose. Connexins and aquaporins play essential roles in maintaining lens homeostasis and transparency and there is a close physical and functional relationship between these two proteins. Aquaporin 0 (AQP0), in addition to its role in water transport in the lens, acts as a cell–cell adhesion molecule. Recently, we showed a new role of connexin (Cx) 50 in mediating cell–cell adhesion. However, the cooperative roles of these two proteins in the lens in vivo have not been reported.

Methods. We generated an AQP0/Cx50 double knockout (dKO) mouse model. Light, fluorescence, transmission thin section, and freeze-fracture electron microscopy, as well as wheat germ agglutinin and phalloidin labeling were used to evaluate lens structure. Mechanical properties of lenses were determined by mechanical compression testing.

Results. DKO mice exhibited small eyes and lenses with severe cataracts, along with lens posterior defects, including posterior capsule rupture. The dKO mouse lenses had severe structural disruption associated with increased spaces between lens fiber cells when compared with wild-type lenses or lenses deficient in either Cx50 or AQP0. DKO mice also exhibited greater reduction in lens size compared with Cx50 KO mice. Gap-junction plaque size was greatly decreased in cortical fiber cells in dKO mice. Moreover, lens stiffness and elasticity were completely diminished, exhibiting a gelatinous texture in adult dKO mice.

Conclusions. This novel mouse model reveals that Cx50 and AQP0 play an important role in mediating cell–cell adhesion function in the lens fiber cells and their deficiency impairs lens fiber organization, integrity, mechanical properties, and lens development.

Keywords: connexin, aquaporin 0 and mouse models

The lens is an avascular organ with a uniquely organized structure, which is formed by anterior epithelial cells and highly differentiated, elongated fiber cells. Epithelial cells located at the lens equator differentiate to lens fiber cells, which gradually lose their intracellular nuclei and organelles in lens development. The ends of elongated fiber cells meet at the anterior and posterior polar axis of the lens to form a suture. During this process, mature lens fibers accumulate high concentrations of AQP0, crystallins, Cx46, and Cx50. AQP0, also known as major intrinsic protein (MIP), is the most abundant membrane protein expressed in lens fibers. However, unlike other members of the aquaporin family, water permeability of AQP0 is low, estimated to be 40 times lower than that of the AQP1 channel in lens anterior epithelial cells.[1] Besides functioning as a water channel, AQP0 plays a crucial structural role as an adhesion molecule in mediating the formation of thin junctions between lens fibers.[2–5] In addition, AQP0 interacts with several proteins, such as calmodulin,[6] the intermediate filament proteins filensin and CP49,[7] as well as γ-crystallins.[8,9]

Microcirculation system, which helps transport nutrients into lens fibers and excrete metabolic waste out, is reliant on an extensive network of gap-junction intercellular communication to maintain lens homeostasis.[10] Gap junctions that connect the cytoplasm of adjacent cells and permit passage of metabolites, ions, and second messengers play essential roles in lens homeostasis and clarity. Gap junctions are formed by a family of membrane proteins, called connexins. Three major connexins have been identified in the vertebrate lens, Cx43, Cx46, and Cx50. Mutations of Cx46 (*Gja3*) and Cx50 (*Gja8*) genes are common causes of congenital cataracts in humans and similar lens cataract phenotypes are also seen in connexin-deficient murine models.[11,12] Cx50 is also involved in lens development and Cx50 knockout (KO) leads to microphthalmia.[13,14] Our previous studies have shown that Cx50, but not Cx46 or Cx43, directly interacts with aquaporin 0 (AQP0) in differentiating lens fibers in the embryonic and young lens, which promotes gap-junctional channel activity.[15–17] Recently, we show that Cx50, unlike two other lens connexins, Cx43 and Cx46, exhibits cell-adhesion function, and this function appears to be independent of its role in forming gap junctions. Moreover, the cell–cell adhesion mediated by Cx50 is involved in lens epithelial–fiber cell differentiation.[18]

These observations imply that these additional roles of Cx50 and AQP0 in cell adhesion may likely help maintain the structural integrity of lens fibers. However, the potential involvement of Cx50 in safeguarding lens fiber structures and maintaining lens integrity in vivo remains largely elusive. We generated Cx50 and AQP0 double-deficient mice to determine the physiologic roles of these two proteins in lens in vivo. In this study, we showed that double KO (dKO) lenses presented with various lens defects, from different extents and severity of lens cataracts to smaller lens sizes and disorganized lens structures with numerous intercellular spaces between fibers. Moreover, the material stiffness of the lens was completely lost. These studies suggest that cell adhesion by these two proteins are likely to play a critical role in maintaining lens fiber organization and integrity.

Materials And Methods

Materials

Rabbit anti-AQP0 polyclonal antibody was obtained from (Alpha Diagnostics, San Antonio, TX, USA). Paraformaldehyde (PFA, 16%) was obtained from Electron Microscope Science (Fort Washington, PA, USA). Wheat germ agglutinin (WGA) and phalloidin were purchased from (Thermo Fisher Scientific, Carlsbad, CA, USA). All other chemicals were obtained from either Sigma-Aldrich (St. Louis, MO, USA) or Fisher Scientific (Pittsburgh, PA, USA).

Generation of dKO Mice Deficient in Both Cx50 and AQP0

The breeding pairs of AQP0KO mice were generously provided by Alan Shiels at Washington University School of Medicine. The dKO mice deficient in both Cx50 and AQP0 , Cx50 (–/–) AQP0 (–/–), were generated by crossing C57BL/6 Cx50 (–/–) mice[13] with C57BL/6 AQP0 (–/–) mice.[19] Genotyping was performed by PCR techniques using genomic DNA isolated from mouse tails and corresponding primers synthesized at the University of Texas Health Science Center at San Antonio's (UTHSCSA) DNA Core Facility. All mice were maintained in a pathogen-free environment at the Association for Assessment and Accreditation of Laboratory Animal Care–accredited UTHSCSA animal facility following the National Institutes of Health Guidelines for the Care and Use of Laboratory Animals. All animals were handled in accordance with the ARVO Statement for the Use of Animals in Ophthalmic and Vision Research and institutional protocols. The animal experimental protocols were approved by the Institutional Animal Care and Use Committee (IACUC). The experiments were conducted blindly without revealing the information of wild-type (WT) and KO mouse models, and identity of the mice became available after completion of the data analysis.

Measurements of Eye Size and Pupil Size

All mice were euthanized in accordance with IACUC guidelines. Eyeballs were carefully dissected and kept in 37°C, prewarmed PBS. Photos were taken with pupil facing up by using a standard dissection microscope. The diameters of pupils and eyeballs at the equator were measured using ImageJ software (http://imagej.nih.gov/ij/; provided in the public domain by the National Institutes of Health, Bethesda, MD, USA). Photos were taken of isolated lenses with anterior side facing down. Lens size diameters were measured with ImageJ.

Lens Tissue Paraffin Sections and Hematoxylin and Eosin Staining

A small incision on the eyeball at the side of optic nerve was made with the assistance of a dissection microscope to remove the lens without any damage. Isolated lenses were kept in PBS at 37°C while photographic images were acquired using a dissecting microscope. For histologic study, isolated lenses were fixed in 4% PFA at room temperature for 2 hours, dehydrated with ethanol and xylene, embedded in paraffin, and cut sagittally in 3-μm thick sections. The tissue sections were mounted to glass slides, stained with hematoxylin and eosin (H&E) and observed under a Keyence microscope (Osaka, Japan). Images were recorded using an Olympus camera (Tokyo, Japan).

Frozen Lens Tissue Sections and Confocal Fluorescence Microscopy

Mouse lenses were isolated and fixed in 2% PFA for 2 hours at room temperature, washed with PBS, immersed in 30% sucrose, placed at 4°C overnight and then embedded in OCT (Sakura, Torrance, CA, USA). Sagittal sections (10 μm) were cut with a cryostat and stained with WGA-conjugated Alexa Fluor 594 (1:400 dilution) for 40 minutes at room temperature, phalloidin-conjugated Alexa Fluor 488 (1:400 dilution) for 40 minutes at room temperature, and 4′,6-diamidino-2-phenylindole (DAPI; 0.2 μg/mL) for 5 minutes at room temperature. The sections were observed, and images were taken with a Zeiss LSM710 laser scanning confocal microscope (Zeiss Inc., Thornwood, NY, USA).

Thin-Section and Freeze-Fracture Electron Microscopy and Quantitative Analyses

Freshly isolated postnatal days (P) 4, 14, and 30 mouse lenses were fixed in an improved fixative containing 2.5% glutaraldehyde, 0.1 M cacodylate buffer (pH 7.3), 50 mM L-lysine, and 1% tannic acid for 2 hours at room temperature as previously described.[20] Each lens was then mounted on a specimen holder with superglue and cut into 200-μm slices with a vibratome. Each lens was carefully oriented on the specimen holder such that either equatorial or sagittal sections of cortical fibers could be obtained initially with a vibratome. Lens slices were then postfixed in 1% aqueous OsO_4 for 1 hour at room temperature, rinsed in dH_2O, and stained with 0.5% uranyl acetate in 0.15 M NaCl overnight at 4°C. Tissue slices were dehydrated through graded ethanol and propylene oxide and embedded in Polybed 812 resin (Polysciences, Warrington, PA, USA). Thick sections (1 μm) cut with a diamond knife were stained with 1% toluidine blue and examined with a light microscope to select the area of interest. Thin sections (80 nm) were cut with a diamond knife, stained with 5% uranyl acetate followed by Reynold's lead citrate and examined in a JEOL 1200EX electron microscope (JEOL, Peabody, MA, USA).

For freeze-fracture electron microscopy, freshly isolated lenses of WT and various KO mice were fixed in 2.5% glutaraldehyde in 0.1 M cacodylate buffer (pH 7.3) at room temperature for 2 to 4 hours. After washing in buffer, lenses were orientated to obtain sagittal (longitudinal) sections with a vibratome, and slices were collected, marked serially from superficial to deep and kept separately. The slices were then cryoprotected with 25% glycerol in 0.1 M cacodylate buffer at room temperature for 1 hour and processed for freeze-fracture electron microscopy according to our routine procedures.[21] Briefly, a single lens slice was mounted on a gold specimen carrier and frozen rapidly in liquefied Freon 22 and stored in liquid nitrogen. Cryofractures of frozen slices were made in a

Investigative Ophthalmology & Visual Science

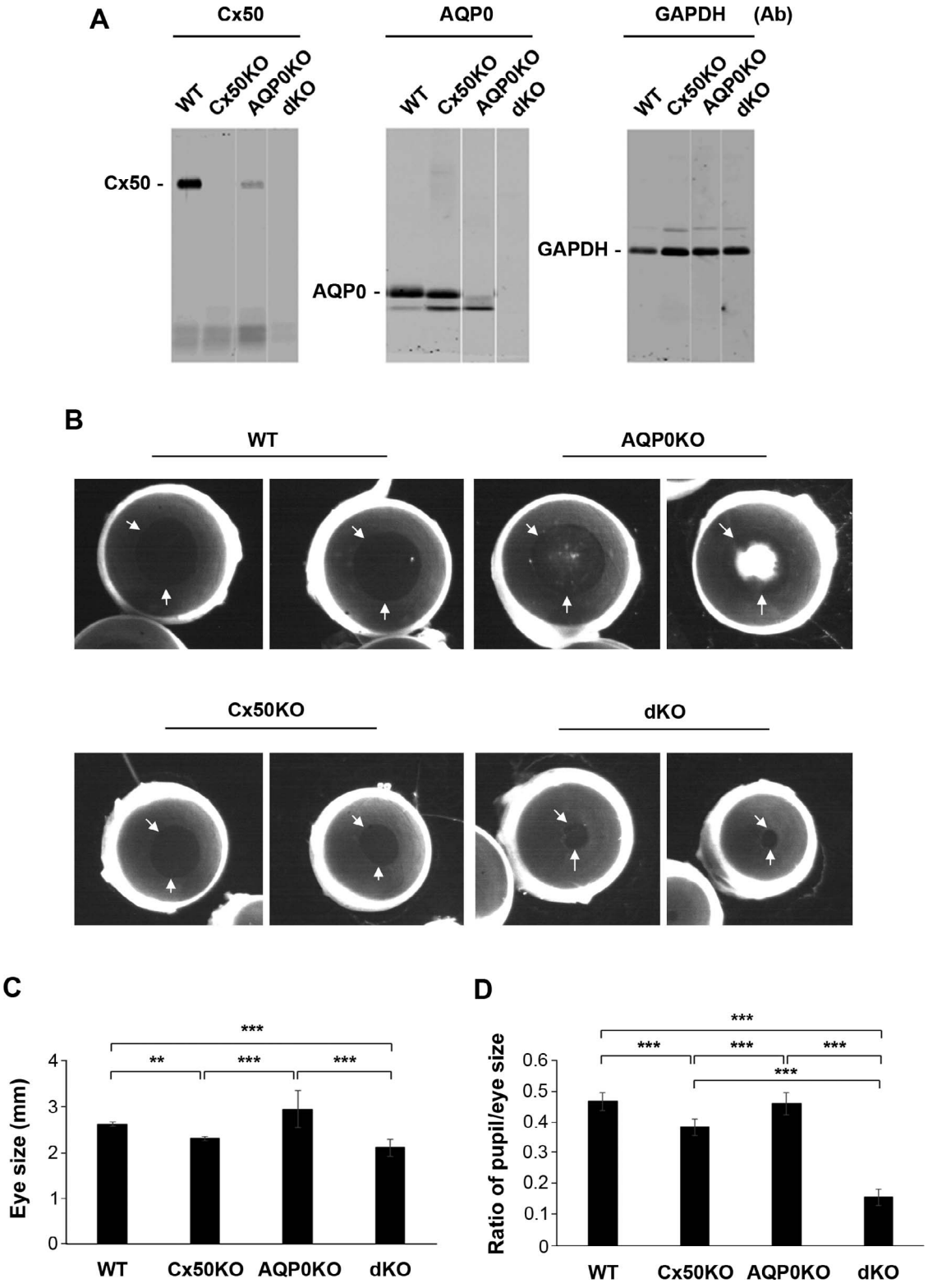

Figure 1. Mice deficient in both Cx50 and AQP0 showed small eye size and abnormally decreased pupil size. (**A**) Lens lysates isolated from WT, Cx50, and AQP0 single KO and dKO mice were immunoblotted with anti-Cx50 (*left*), AQP0, or glyceraldehyde 3-phosphate dehydrogenase antibody. (**B**) The eyeballs of WT, Cx50, and AQP0 KO and dKO were carefully dissected, kept in 37°C prewarmed PBS and imaged. The *white arrows* indicate the pupils. (**C**) Eye size was measured along the equator of eyeball. (**D**) The pupil size was measured and the ratio of pupil size versus eye size was calculated. All the data are presented from 3-months old as mean ± SEM. $^{**}P < 0.01$; $^{***}P < 0.001$. $n \geq 8$.

Investigative Ophthalmology & Visual Science

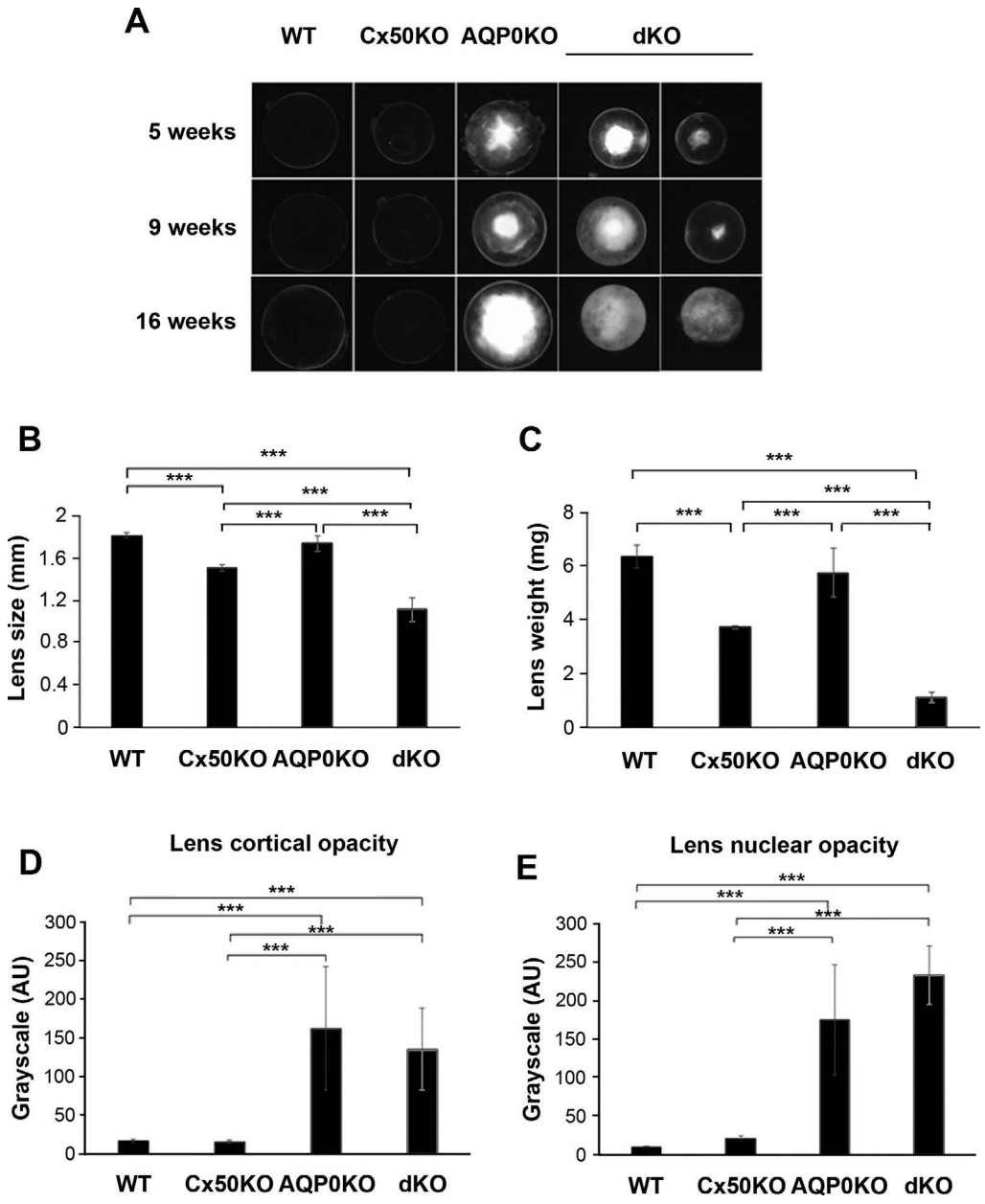

FIGURE 2. Lens deficient in both Cx50 and AQP0 shows heterogeneous, severe cataracts. (**A**) The optical images of lenses from 5-, 9-, and 16-week-old WT or KO mice deficient in Cx50, AQP0, or both Cx50 and AQP0. The images were taken at the identical magnification. The diameter (**B**) and weight (**C**) of 3-month-old lenses of WT and Cx50 and AQP0 single and dKO mice were determined. The magnitude of cataracts in cortical fibers (**D**) and nuclear fibers (**E**) formed in 3-month-old WT or KO mice was measured and quantified by ImageJ integrated density in corresponding lens area. All the data are presented as mean ± SEM. $^{***}P < 0.001$. $n \geq 5$.

modified Balzers 400T freeze-fracture unit (Balzers AG, Balzers, Liechtenstein), at a stage temperature of −135°C in a vacuum of approximately 2×10^{-7} Torr. The lens tissue was fractured by scraping a steel knife across its frozen surface to expose fiber cell membranes. The fractured surface was then immediately replicated with platinum (~2-nm thick) followed by carbon film (~25-nm thick). The replicas, obtained by unidirectional shadowing, were cleaned with household bleach and examined with a JEOL 1200EX TEM. Freeze-fracture replica immunogold labeling was performed based on our published procedures.[21] Briefly, freshly isolated lenses of dKO mice were lightly fixed in 0.75% PFA in PBS for 30 to 45 minutes at room temperature, and then cut into 300-μm slices with a vibratome to make freeze-fracture replicas. One drop of 0.5% parloidion in amyl acetate was used to secure the integrity of the whole piece of a large replica during cleaning and immunogold labeling procedures. The replica was digested with 2.5% SDS, 10 mM Tris-HCl, and 30 mM sucrose, pH 8.3 (SDS buffer) at 50°C until all visible attached tissue debris was removed from the replica. The replica was then rinsed with PBS, blocked with 4% BSA-0.5% teleostean gelatin in PBS for 30 minutes, and incubated with rabbit anti-Cx46 antibody (Santa Cruz Biotechnology, Dallas, TX, USA) at 1:10 dilution for 1 hour at room temperature. The replica was washed with PBS and incubated with 10 nm Protein A gold (EY Laboratories, San Mateo, CA, USA) at 1:50 dilution for 1 hour at room temperature After rinsing, the replica was fixed in 0.5% glutaraldehyde in PBS for 10 minutes, rinsed in water, collected on a 200-mesh Gilder

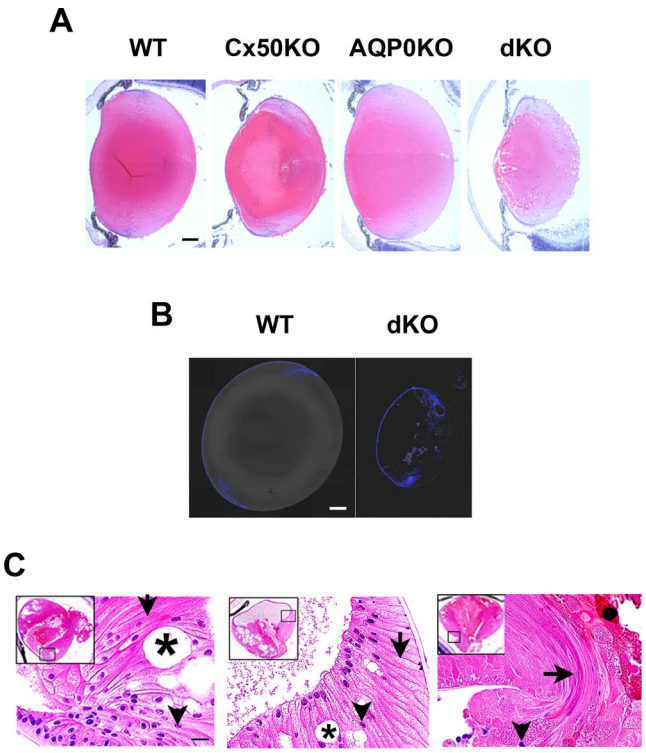

Figure 3. Lens deficient in both Cx50 and AQP0 show distorted fiber structure, cell nuclei distribution, and increased intercellular spaces in lens fiber cells. (**A**) Images of midsagittal paraffin tissue sections of lenses from WT or KO mice deficient in Cx50, AQP0, or both Cx50 and AQP0 mice at P4. (**B**) Frozen tissue sections of lens isolated from postnatal day 15 WT and dKO mice were DAPI labeled and imaged. (**C**) Images of midsagittal paraffin tissue sections of three examples of postnatal day 15 dKO lenses are shown at higher magnification. The locations are indicated in the frames of insert images at low magnification. Intercellular space (*asterisks*), central nuclei (*arrowheads*), disordered and swelling fibers (*arrows*), and liquefaction necrosis (*circles*) are indicated. *Scale bar*: 200 μm in (**A**) and (**B**), and 20 μm in (**C**).

finder grid, rinsed with 100% amyl acetate for 30 seconds to remove parloidion and viewed with a JEOL 1200EX TEM. The size of gap junctions was measured with the Zeiss AxioVision LE 4.4 on PC. The percentage of cell membrane area specialized as gap junctions was calculated from micrographs taken from three individual replicas as previously described.[21]

Tissue Preparation for Mechanical Testing and Data Analysis

Carefully dissected lenses were placed in PBS. Lens damage was assessed under a dissection microscope. If any damage was detected after dissection, the lens was discarded. The genotypes used included WT and KO, including Cx50, AQP0, and Cx50/AQP0 dKO. A lens compression test was used to characterize the mechanical properties of encapsulated lens. Once the sample was ready for testing, it was placed in a clear testing chamber with 8 mL of PBS and loaded onto the compression apparatus for mechanical testing. Compression testing was carried out with a custom machine with a steel top plate, which contacts the lens during the experiment.[22] The motor movements and data acquisition are controlled by interfacing MATLAB (MathWorks, Natick, MA, USA) with GalilTools software (Galil, Rocklin, CA, USA). Once the sample was prepared, the testing container was placed directly on the load cell (LSB 200, 50 g; Futek, Irvine, CA, USA) where images of the lens are taken with a camera (D300s; Nikon, Melville, NY, USA) outfitted with a macro bellows (PB-6; Nikon), which increases the imaging system's resolution for determining the shape of the lens. Before compression testing began, the camera was calibrated with a steel ball bearing with a diameter of 4.75 mm. On average, calibration yielded a spatial resolution of approximately 2 μm/pixel.

After the lens was imaged, the top plate descended with a velocity of 250 μm/s until a contact force of 0.5 mN was measured, indicating contact with the lens. Then, a preprogrammed loading protocol was applied to the lens. Force and displacement data were collected throughout the duration of the compression test, which comprised two stages. The first stage of the compression program is the preconditioning phase, which has three loading/unloading cycles at three different strain values (2.5%, 5%, 7.5%) at a strain rate of 2% of axial thickness per second.[22] The second stage of the program is the experimental loading portion and is composed of three loading cycles to the peak percent strain value of 10.

Force (F) and displacement (d) data from the first 10% strain loading ramp were smoothed with a moving average filter in MATLAB, then fitted with a modified Hertz model of the form

$$F = \frac{4}{3} \cdot \frac{E}{1 - \nu^2} \cdot \sqrt{R} \cdot d^b, \quad (1)$$

where E is the effective elastic modulus, ν is the Poisson ratio (assumed equal to 0.5), R is the radius of curvature, b is an exponent describing the degree of material nonlinearity, and d is the displacement (mm) of the top plate relative to its point of contact on the lens. Note that in the original Hertz model, b = 1.5 for a linear elastic material. Resilience was calculated by dividing the area underneath the unloading curve by the area underneath the loading curve. The geometry of the unloaded lens, including its axial thickness, equatorial diameter, and radius of curvature R, was characterized using digital image processing in MATLAB.

Statistical Analysis

All data were analyzed with GraphPad Prism 5 Software (GraphPad Software, La Jolla, CA, USA). When significant difference was found in the data by the ANOVA, the post hoc Tukey tests of significance was used to further compare group differences. The data were presented as the mean ± SEM of at least three measurements. Statistical significance was designated for analyses with $P < 0.05$. Asterisks in all figures indicate the degree of significant differences compared with controls ($^*P < 0.05$; $^{**}P < 0.01$; $^{***}P < 0.001$).

Results

Cx50- and AQP0-Deficient Mice Exhibit Small Pupil Size, Highly Heterogeneous Lens Opacities, and Small Eye Phenotypes

To explore the functional importance of Cx50 and AQP0 in the lens in vivo, we deleted Cx50 and AQP0 by crossing individual-gene KO mice[13,19] to generate Cx50 and AQP0 dKO mice. The genotype of dKO mice was confirmed by PCR with specific primers (data not shown) and confirmed by Western blots. Western blots with Cx50 or AQP0 antibody showed the deletion of corresponding proteins and dKO showed the disappearance of both Cx50 and AQP0 (Fig. 1A). Interestingly, deletion of AQP0 (AQP0KO) greatly reduced the expression of Cx50, whereas Cx50KO had a lesser effect on AQP0 levels. The fast migrating band shown in Figure 1A, the middle panel is

Investigative Ophthalmology & Visual Science

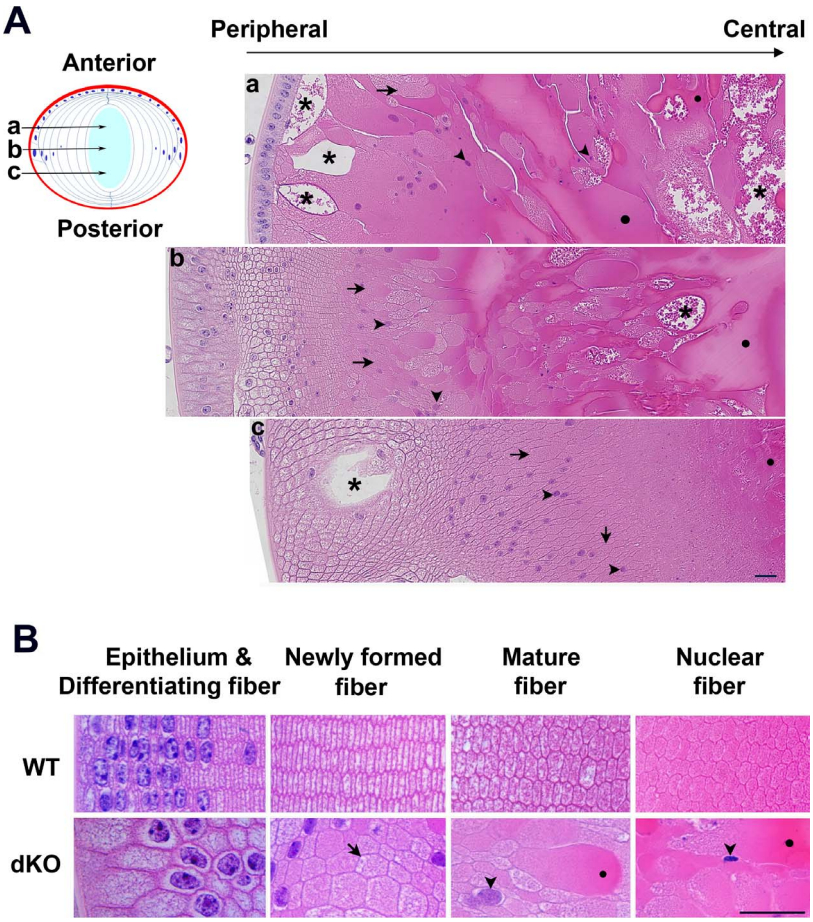

Figure 4. DKO lenses exhibit distorted fiber structure, abnormal cell nuclei distribution, and increased intercellular spaces in lens fibers. Image of coronal paraffin sections of postnatal day 15 dKO mouse lenses at three depth levels as indicated by a, b, and c in the diagram (**A**). Representative images of lens at various regions (**B**). Intercellular space (*asterisks*), central nuclei (*arrowheads*), disordered and swelling fibers (*arrows*), and liquefaction necrosis (*circles*) are indicated. *Scale bar*: 20 μm.

unlikely an AQP0 product, but an unspecific protein, given this band was also shown in AQP0KO. However, the upper band with the expected molecular weight only showed in WT and Cx50KO, not in AQP0KO and dKO. The eyeball size of Cx50KO and dKO mice was decreased significantly compared with WT and AQP0KO mice. Compared with the Cx50KO eyeball, the dKO eyeball size was slightly decreased, but not at a significant level. The size of eye pupils in dKO mice was disproportionally smaller than that of Cx50KO, AQP0KO, and WT mice (Fig. 1B). Although Cx50 and dKO eyeball size was comparable, the pupil size of dKO mouse eyeballs was significantly smaller than that of Cx50KO (Figs. 1C, 1D). The severity of dKO cataracts appeared to be less severe than that of AQP0 mice (Fig. 1B). Except eye phenotypes, we did not observe any other changes in dKO as compared with WT mice, including viability, fertility, and body mass at the identical age.

When dissecting lenses from dKO mice, we found that dKO lenses were very fragile and difficult to isolate fully intact, which was different from WT and Cx50 and AQP0 single KO lenses. Cx50 KO shows the reduction of lens diameter.[13] dKO resulted in the smallest lens size, even significantly smaller than Cx50 KO lenses (Fig. 2B). Lens weight comparisons followed a similar pattern as the lens size with more noticeable differences particularly in the dKO (Fig. 2C). We then compared lens opacity of dKO with Cx50 and AQP0 KO lenses. Lenses deficient in both Cx50 and AQP0 exhibited comparable degrees of lens opacity as compared with AQP0KO while Cx50 deficiency exhibited mild cataracts as previously reported (Figs. 2A, 2D, 2E). In contrast to condensed cataracts observed in AQP0-deficient lens, opacity in dKO lenses appeared to be heterogeneous and diffused, ranging from incipient nuclear opacity, cortical opacity, and subcapsule opacity to whole-lens opacity. Quantification of integrated intensity of cataracts in both cortical and nuclear regions revealed the most dramatic magnitude with deficiency of AQP0 lenses regardless of Cx50 expression level (Figs. 2D, 2E). These data suggest that deletion of both Cx50 and AQP0 have major impacts on lens size and patterns of lens opacities.

Deficiency of both Cx50 and AQP0 Leads to Enlarged Intercellular Spaces and Disruption of Lens Fiber Organization and Nuclei Distribution

We examined morphologic changes in lenses from Cx50/AQP0 dKO mice in comparison with single-gene KO or WT control lenses at various stages of lens development using H&E staining, fluorescence labeling, and electron microscopy. Morphologic abnormalities were first observed at P4 in dKO lens. H&E staining of mouse lenses showed that compared to the single-gene KO lenses, Cx50/AQP0 dKO were not only the smallest in lens size, but also exhibited enlarged intercellular spaces in the anterior and posterior regions of the lens (Fig. 3A). At P15, great alterations of lens morphology were

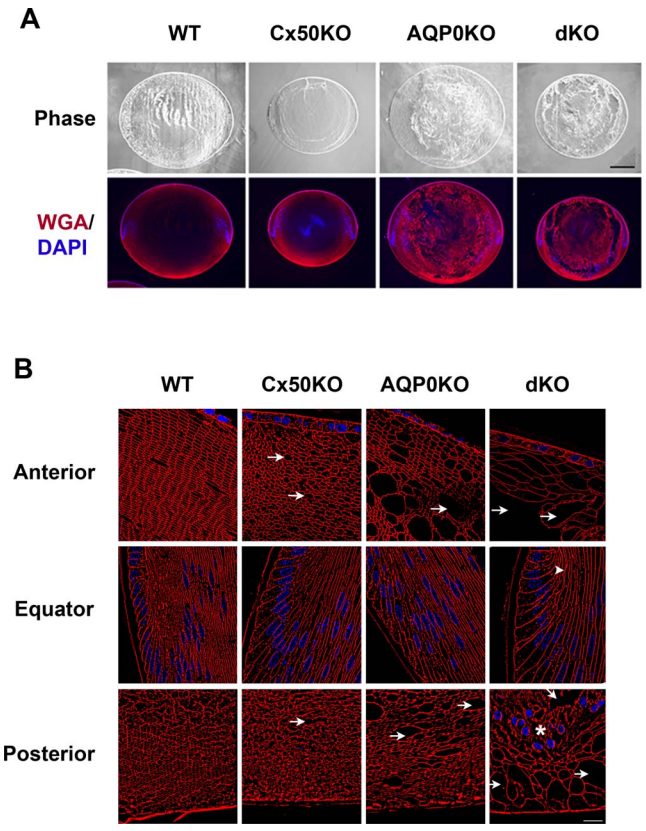

Figure 5. Disorganization of fiber cell morphology in lens deficient in Cx50 and AQP0. Frozen-lens tissue sections of postnatal day 15 mouse lenses of WT or KO mice deficient in Cx50, AQP0, or both Cx50 and AQP0 were stained with Alex594-conjugated WGA and counter-stained with DAPI. The phase and fluorescence images were taken by confocal microscopy at low magnification (**A**, *scale bar*: 200 μm) and high magnification at the anterior, equator and posterior regions of the lens (**B**, *scale bar*: 20 μm). Intercellular spaces (*asterisks*), central nuclei (*arrowheads*), and disordered fibers (*arrows*) are indicated.

observed in dKO lenses, such as abnormal nuclei distribution, various sized intercellular spaces, disorganized fiber structures, and liquefaction necrosis, particularly close to the center of lens (Figs. 3C, 4A, 4B). The abnormal nuclei distribution was observed throughout the entire lens fibers. In Figure 3B, contrary to majority of nuclei distributed along lens equator region in WT, the distribution pattern of cell nuclei in the dKO lenses was abnormally present in the central as well as posterior parts of lens (Fig. 3B). In addition, disorganized differentiating and swelling mature fibers were observed in the dKO lenses (Fig. 3C). Large liquefied areas were also observed in dKO lenses as shown in the Figure 3C, left and middle panels, which appeared to push anterior ends of fibers apart. In dKO lenses, ends of lens fibers aligned in parallel instead of connecting end-to-end to form the lens anterior suture (Fig. 3C, left and middle panels) and posterior suture (Fig. 3C, right panel). Moreover, lens fibers extruded from the posterior lens capsule ruptured (Fig. 3C, right panel).

Coronal sections of dKO lens showed disordered fiber structures with enlarged intercellular spaces and liquefied areas primarily at subcortical and central regions of dKO lenses (Fig. 4). Distorted structures started anteriorly, right beneath the single layer of epithelial cells. At the lens equator region, epithelial cells and actively differentiating fibers aligned abnormally, were larger than WT, but overall differentiating fiber cell structure did not have any apparent abnormalities. However, the apparent disruption increased toward the lens core, exhibiting distorted, swelling lens fiber cells and enlarged intercellular spaces. Posteriorly, the appearance of large intercellular spaces was present in the region of differentiating lens fibers. Different sized intercellular spaces were distributed throughout dKO lenses as shown in the representative images of lens sections (Fig. 4A, 4B). Additionally, increased liquidized areas were observed toward the mature and nuclear fibers (Fig. 4B).

The organization of lens fibers was further studied by labeling lens tissue sections with a cell membrane marker, WGA, and counter-staining with DAPI for nuclei. An overall loss of lens fiber membrane structure was observed; especially in the Cx50/AQP0 dKO lenses (Fig. 5A). When examining individual sections of the lens, there was some loss of fiber structures within the anterior and posterior lens regions in the AQP0KO animals, which became more evident in the Cx50 and the most in AQP0dKO lens (Fig. 5B, upper and lower panels). Conversely, most of the cell organization was preserved around the lens equator (bow) region, except for the elongated lens cells underneath the epithelial cells in dKO lenses (Fig. 5B, middle panels). These data suggest that Cx50 and AQP0 play an important role in maintaining the integrity and organization of lens fibers.

We investigated the microscopic organization of lens fiber cells in dKO mice. Thin-section electron microscopy revealed the presence of numerous intercellular spaces between the lens fiber cells (arrows indicate cell borders) in both AQP0 and Cx50 single KO, and which appeared to be more extensive in the dKO lens (Fig. 6A). Freeze-fracture microscopy was performed to determine the size of junctional plaques (Fig. 6B). Based on our previous published protocol,[21] we quantified the gap-junction size distributions of WT, Cx46, Cx50, and AQP0 single KO and Cx50/AQP0 dKO (Fig. 6C). WT superficial fibers contained the three size–range gap-junction plaques for which the large-size group was within 0.3 to 2.86 μm^2, the medium-size group was within 0.1 to 0.29 μm^2, and the small-size group was within 0.01 to 0.09 μm^2. Three replicas prepared from three mouse lenses for each genotype were used for the measurements. Cx46KO[23] superficial fibers contained mostly the large gap-junction plaques (a total of 123 gap-junctional plaques were measured), suggesting that Cx50 was the key connexin in these large gap-junction plaques observed. Cx50KO superficial fibers contained mostly the small and some medium sizes gap-junction plaques (a total of 179 gap-junctional plaques were measured). Like WT, AQP0KO superficial fibers contained the three size–range gap-junction plaques (a total of 383 gap-junctional plaques were measured) as those of WT (a total of 356 gap-junctional plaques were measured). Interestingly, Cx50/AQP0 dKO superficial fibers contained only the small size gap-junction plaques (a total of 136 gap-junctional plaques were measured). To confirm the presence of small size plaques formed by Cx46, immunogold labeling on freeze-fracture replicas was performed and the result showed specific localization of Cx46 antibody on all small gap-junction plaques as represented by 10-nm gold particles in Cx50/AQP0 dKO superficial fiber cells (right panel, Fig. 6B). These results suggest the possibility of Cx50 and AQP0 interaction, with the capacity of forming large junctional plaques, which may help stabilize lens fiber structures. Together, these data support an important role of both Cx50 and AQP0 in maintaining structural integrity and compact organization of lens fibers.

Loss of Tissue Stiffness in Cx50 and AQP0 dKO Lens

Given the disrupted lens fiber organization and integrity, we expected to observe significant alterations of physical proper-

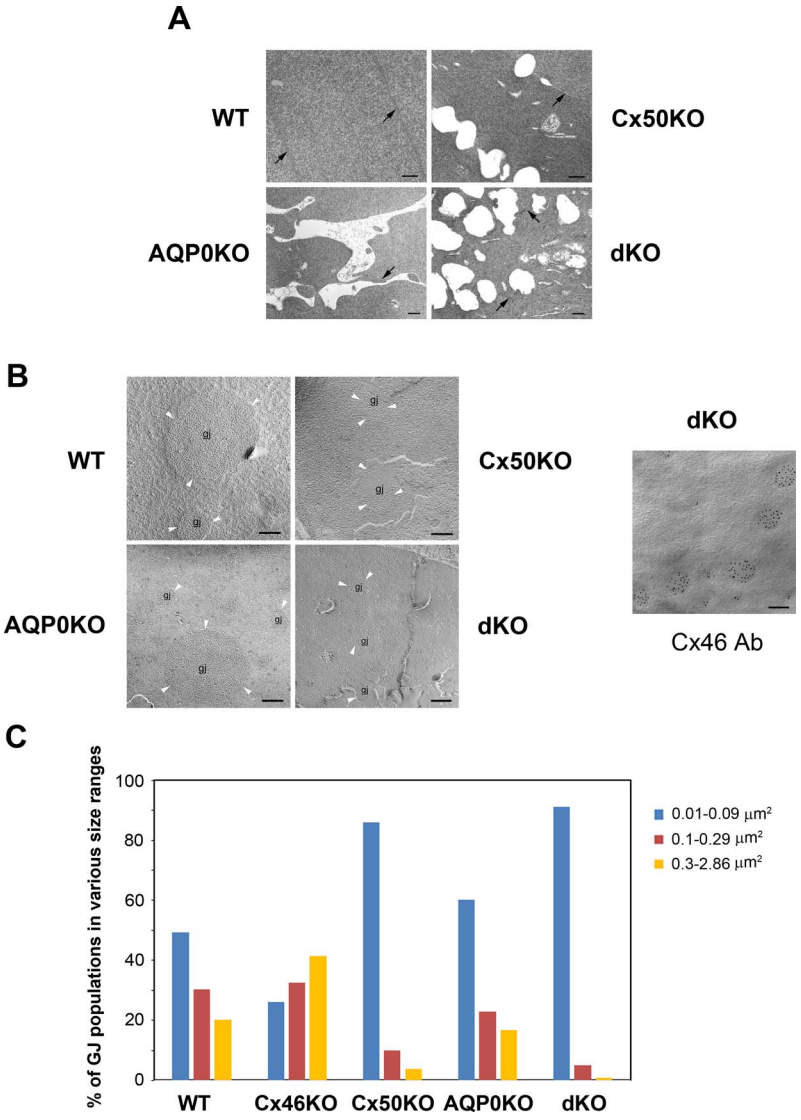

Figure 6. Electron microscopy shows the presence of intercellular spaces in lens fibers and a decreased size of gap-junction plaques. (**A**) One-month-old mouse lenses of WT, Cx50, and AQP0 single- or double-gene KO mice were processed for thin-section TEM. Representative images from the anterior superficial cortex of the lenses show that cortical fiber cells exhibit the intact cell membranes (*arrowheads*) in WT (**A**), but display enlarged intercellular spaces of various sizes in single KO lenses for Cx50, AQP, and in a dKO lens for AQP0 and Cx50. Several short, intact cell membranes (*arrows*) were also observed among these enlarged spaces. All *scale bars*: 500 nm. (**B**) Freeze-fracture microscopy was performed with 1-month-old lens of WT, Cx50, and AQP0 KO and dKO mice. Representative images are shown and gap-junctional plaques are indicated as "gj" and *white arrowheads*. Immunogold labeling against Cx46 of freeze-fracture replicas was performed using 10-nm gold particles (*right panel*). *Scale bars*: 200 nm. (**C**) Quantitative analysis of percentage of gap-junction (GJ) population in various size ranges in WT, Cx46KO, Cx50KO, AQP0KO, and dKO. Small size GJs are approximately 0.01 to 0.09 μm^2; middle size GJs are approximately 0.1 to 0.29 μm^2; and large size GJs are approximately 0.3 to 2.86 μm^2.

ties in the dKO lens. Tissue compression testing was conducted for 1- and 4-month-old WT and three KO mouse models (Fig. 7). For 1-month-old mice, dKO lenses generated so little force when compressed and the generated data were below the limit of detection of the load cell (<100 μN). In addition, linear regression found no correlation between lens size and effective elastic modulus, presumably due to the use of the modified Hertz model, which accounted for lens size. For 4-month-old mice, statistical analysis yielded significant differences between WT, AQP0 KO, Cx50 KO, and Cx50/AQP0 dKO lenses. WT and Cx50 had similar resiliencies. These results suggest that dKO completely loses stiffness and elastic properties of the lens, which is in accordance with severe disruption of lens fiber organization and integrity. The effective modulus for each genotype was significantly higher at 4 than at 1 month.

Discussion

Integrity and precise organization of lens fiber structures are crucial for light transmission and optical quality.[24] In this study, we generated a dKO mouse model deficient in lens specific Cx50 and AQP0 expression. Here we demonstrate that deficiency of both Cx50 and AQP0 leads to a significant distortion of lens fiber organization and integrity, reduced lens size with severely diffuse cataracts resulting in a complete loss of lens elasticity. The significance of these findings includes the following aspects: (1) this is the first study reporting the

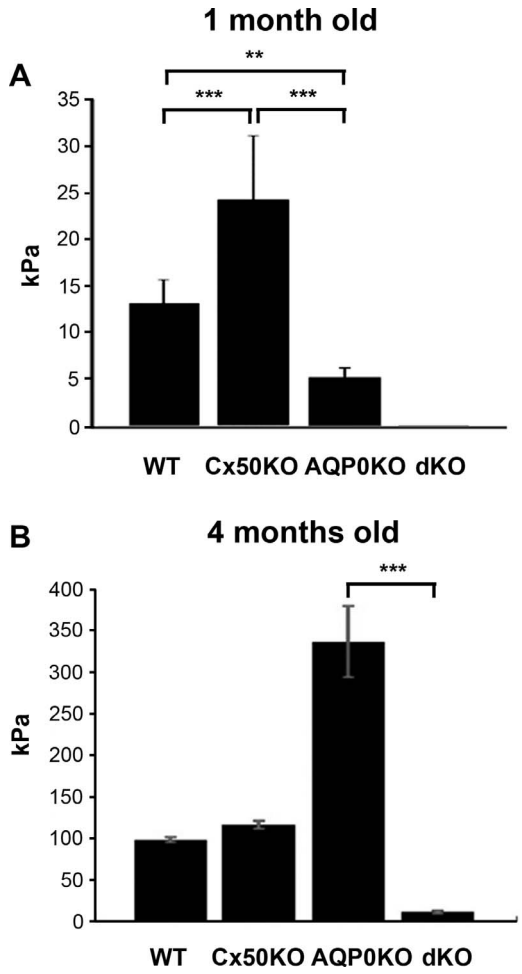

FIGURE 7. Four-month-old lenses deficient in Cx50 and AQP0 completely lose tissue stiffness. Lenses were isolated from 1- and 4-month-old WT and Cx50 and AQP0 single and dKO mice. Lens stiffness was measured by tissue compression testing for (**A**) 1- and (**B**) 4-month-old lenses. Compared with WT controls, $n \geq 6$, data are presented as mean ± SEM. $^{**}P < 0.01$; $^{***}P < 0.001$. One-month old, $n \geq 15$; 4-month old, $n \geq 6$.

double KO with deficiency of Cx50 and AQP0. Interestingly, we do not observe the further augmentation of the severity of cataracts as the cataracts are the major phenotypes reported in the previous single KO studies. However, we observed severe distortions of lens organization and loss of cell adhesion with a great increase of intercellular spaces. Therefore, this phenotype is likely attributed to loss of the cell-anchoring function, which is crucial for integrity of lens fibers. (2) We have thoroughly examined and compared the lens morphology not only in dKO, but also in single KO using H&E staining, fluorescence labeling, and electron microscopy. (3) We have adopted various techniques to assess the lens structures and material properties, including electron microscopy and lens material stiffness analysis. These drastic phenotypic changes in dKO lenses are likely caused by cell-adhesion function of both proteins.

It was not surprising that major disruptions were present in subcortical fibers but not at bow region as Cx50 and AQP0 expression increases with fiber differentiation. At the bow region, epithelial cells start to differentiation as Cx50 and AQP0 expression increases. In addition to forming water channels, AQP0 is known to be a cell-adhesion molecule and plays an important role in lens-fiber cell architecture.[4,25] Increased intercellular spaces have been reported in lens fibers lacking AQP0.[26] Therefore, in consideration of our data, AQP0 deficiency is responsible for lens-fiber disorganization. We have recently observed a similar phenotype of disorganized fiber structures in Cx50KO mice, although the degree of deterioration was less severe than in AQP0-deficient lenses.[18] This similar disruption of lens fiber organization was also previously reported in lenses expressing cataract-causing mutants of Cx50.[27,28] We recently reported that Cx50, like AQP0, also exhibited a cell adhesion function, and co-expression of these two proteins further enhanced cell-adhesion function.[18] We and others have reported increased spaces between fiber cells and multiple morphologic defects in the cortical fibers of Cx50KO lenses.[18,29] The increased intercellular spaces filled with liquid and cell swelling in dKO are likely caused by impaired water transport function and alteration of hydrostatic pressure attributed both AQP0 and Cx50. In mature lens fibers, AQP0, unlike its distribution in differentiating lens fibers located at broad side of lens fibers, is located predominantly on both short and broad sides of fibers.[30] This transition is associated with the truncation of AQP0 that coincides with the loss of water channel function, switching from functioning as a water channels to forming thin junctions between fiber cells. Cx50, on the other hand, is located on the broad side of fiber cells.[31–33]

Electron microscopy studies show that gap-junction plaques are associated with interlocking ball-and-sockets structure, which is suitable for maintaining fiber-to-fiber stability.[20] Moreover, we show here by freeze-fracture microscopy that Cx50 is involved in forming large gap-junction plaques as evidenced by the large-sized junctional plaques that are present in Cx46 KO lenses as shown in Figure 6C. In Cx50 KO, and especially in dKO mice, small gap-junction plaques were primarily detected. In the WT mouse lens, Cx46 and Cx50 are shown to be colocalized (co-distributed) in a majority of gap-junctional plaques of cortical fiber cells.[34] Previous studies have also shown that in the Cx46-KO mouse lens, many large gap-junction plaques that contain only Cx50 are found in the cortical fiber cells (as seen in the present study, and Refs. 20, 35). This indicates that large gap-junction plaques in WT mouse lenses, the large-sized gap-junction plaques are composed of a larger amount (percentage) of Cx50 and a small amount (percentage) of Cx46 in the cortical fiber cells. Thus, this gives a reasonable explanation that in Cx50KO mouse lenses, after removing Cx50, the remaining small percentage of Cx46 would form mostly small gap-junction plaques as seen in our freeze-fracture data. Furthermore, several previous structural studies[36–38] have demonstrated that AQP0 and connexins are co-localized in gap-junction plaques, especially in the young cortical fiber cells. It is thus conceivable that a large population of small-size gap-junction plaques is expected to be distributed in the lenses of AQP0/Cx50 dKO mice as shown in the present study.

As illustrated in Figure 8, we show that fiber dysmorphology was exacerbated in Cx50/AQP0 dKO lenses with severe distortions and loss of lens fiber structures at various regions within the lens. Cx50 and AQP0 are distributed at different regions of lens fiber cells, this may help anchor cells together at all sides of lens fibers. Deficiency of these two proteins leading to lose fiber cells disassociating from each supports their functional roles as cell-adhesive proteins. In addition, disorganization of lens fibers with loose fiber cells as well as impaired lens physical properties with enlarged intercellular spaces further strengthens a structural and adhesive role of Cx50 and AQP0. The severe structural disruption in dKO, which is moderate in single KOs, implies the synergistic role of Cx50 and AQP0. This phenotype is likely caused by impairment of cell–cell adhesion by both proteins given that

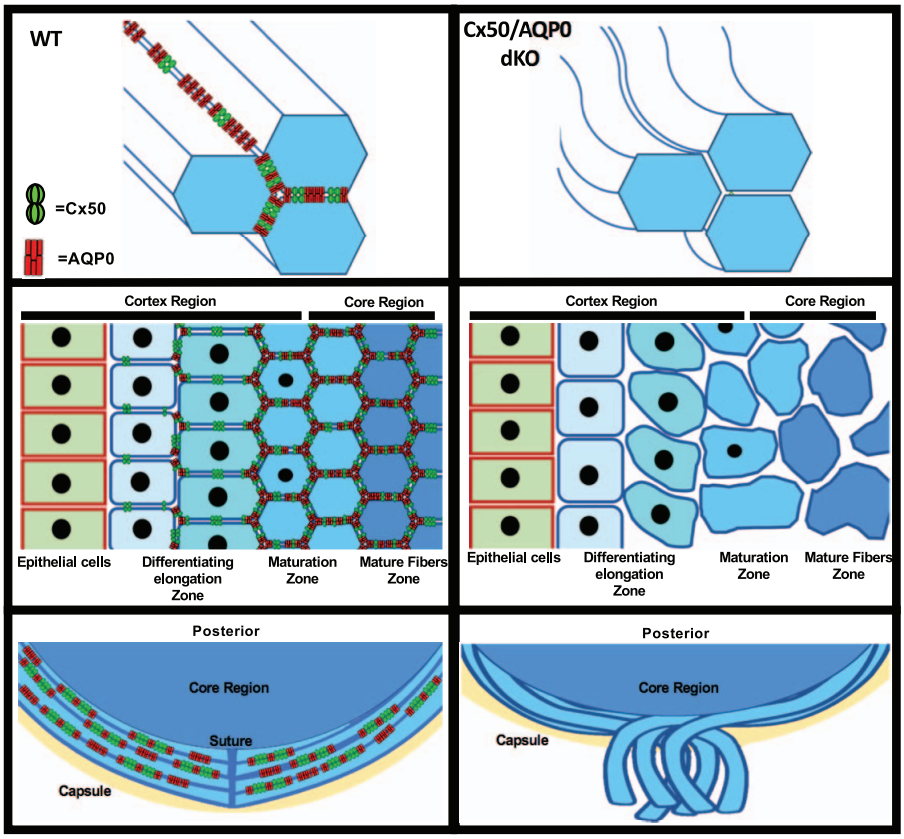

Figure 8. Impairment of cell-adhesion function mediated by Cx50 and AQP0 disrupts the organization of lens fibers. In WT mice, Cx50 and AQP0, located at broad side and short side of lens fibers, respectively, mediate the cell–cell adhesion, which maintains lens fiber integrity (*left upper* and *lower panels*). Deficiency of Cx50 and AQP0 shown in dKO lenses loses cell–cell adhesion, resulting in the alterations of lens structures in various lens regions (*right upper*, *middle*, and *lower panels*). These changes include enlargement of fiber cells in the differentiating elongation zoon, increased intercellular spaces toward the mature fibers and disorganization of lens fibers with abnormal distribution of cell nuclei, which consequently leads to loss of lens tissue elasticity. At the posterior part of lens, newly formed fibers cannot bundle properly toward the core of lens, which leads to lens posterior extrusion.

the extent of cataracts is not augmented in dKO. At this stage, we cannot exclude the possibility of the loss of other functions that may contribute to the phenotypes due to the deficiency of Cx50 and AQP0, such as water transport, cytoskeleton interaction, ball-and-socket formation, and so on. However, cooperative roles of these two proteins play an important role in maintaining lens structure and integrity.

We showed that the magnitude of cataract severity was not significantly worsened in Cx50/AQP0 dKO when compared with AQP0KO lenses; however, the pattern of cataracts appears to be more diffuse in contrast to condensed cataracts formed by AQP0-deficient lens. One possible explanation is, deficiency of Cx50, different from that of the other lens fiber connexin, Cx46, forms relatively minor cataracts, which is in accordance with a relatively minor role of Cx50 in maintaining lens transparency.[13,14] As reported previously, contrary to Cx46, Cx50 plays lesser roles in forming gap junctions and mediating intercellular coupling in the lens nucleus and in transmitting reductant glutathione between mature lens fibers.[39–42] Instead, Cx50 is likely to be involved in mediating cell-adhesion function in mature lens fibers. Secondly, lens organization is severely disrupted with unaligned lens fiber cells and many enlarged intercellular spaces. These structural changes of lens fibers are likely to alter the formation and appearance of cataracts.

Cx50KO mice exhibit smaller lens size.[13,14] The lens size and weight in Cx50/AQP0 double-deficient mice are further reduced compared with Cx50KO. Cx50 plays an important role in lens development and lens epithelial to fiber cell differentiation.[13,43,44] Moreover, cell–cell adhesion is known to be crucial for the process of normal cell proliferation and differentiation. Indeed, we showed disruption of Cx50 adhesion function compromised lens epithelial to fiber differentiation.[18] Interestingly, lens development is not affected by AQP0 deficiency. One plausible reason is that as previously suggested,[30] AQP0 primarily functions as an adhesive molecule in mature lens fibers, but less so in differentiating lens fibers and the latter is mainly responsible for postnatal development and size of the lens. The further reduction of lens size and weight in dKO could be a result of disrupted lens organization, which could extend their impact on both mature and differentiating lens fibers. Indeed, the dKO lens, not only have reduced lens size and weight, but also exhibit dysregulation of the denucleation process with delayed and abnormal distribution of nuclei even with their presence in the posterior region of the adult mouse lens.

Due to the impairment of lens integrity and lens fiber structure, it is not surprising that lens stiffness is completely compromised for 4-month-old dKO lenses. At 1-month old, stiffness of dKO lenses were below level of detection for the load cell. The reduced lens stiffness for 1-month-old mice in AQP0KO compared with WT is consistent with a previous study in which a compression stress test resulted in increased equatorial strain levels in AQP0KO mouse lenses.[26] Interestingly, the stiffness in Cx50KO lenses is even higher than WT. However, 4-month-old adult mice lenses displayed different

physical properties. For example, 4-month-old AQP0KO lenses exhibited the highest levels of stiffness compared with WT, Cx50KO, and dKO groups. The possible reason is that AQP0KO forms condensed cataracts at this age. Although the mechanisms driving age-related changes in lens stiffening are unknown, the increased abnormal level of cross-linked proteins, protein aggregation, cholesterol, and phospholipids during cataract development leads to the increase of lens stiffness as previously reported.[45,46] It is plausible that knocking out Cx50 and/or AQP0 could alter age-related stiffening by altering the type and rates of these interactions. Formation and growth of nuclear cataract in the AQP0KO lens presumably causes the large increase in stiffness between 1 and 4 months of age, overwhelming the loss of fiber cell adhesion–related loss in stiffness in the young lens. The Cx50-null lenses may be stiffer as a result of increased fiber cell packing density (Fig. 5B)—an effect that would be relatively independent of age. Lens stiffness and elasticity of dKO mice appear to be completely lost, which is in accordance with loose-structured lens fibers associated with large intercellular spaces.

Together, this study uncovers a cooperative role of Cx50 and AQP0, two abundant membrane proteins in lens fibers, possibility forming interlocking system. These results indicate a crucial role of both proteins in maintaining structural integrity of fiber cells and lens development.

Acknowledgments

The authors thank Alan Shiels at Washington University School of Medicine for generously providing AQP0 knockout mice, Eduardo Cardenas for critical reading and editing the manuscript, and Hongyun Cheng for technical assistance.

Supported by National Institutes of Health (NIH; Bethesda, MD, USA) Grants EY012085 and Welch Foundation Grant AQ-1507 (JXJ0; Houston, TX, USA), NIH EY013163 (TWW), and NIH EY005314 (WKL).

Disclosure: **S. Gu**, None; **S. Biswas**, None; **L. Rodriguez**, None; **Z. Li**, None; **Y. Li**, None; **M.A. Riquelme**, None; **W. Shi**, None; **K. Wang**, None; **T.W. White**, None; **M. Reilly**, None; **W.-K. Lo**, None; **J.X. Jiang**, None

References

1. Zampighi GA, Kreman M, Lanzavecchia S, et al. Structure of fucntional single AQP0 channels in phospholipid membranes. *J Mol Biol*. 2002;325:201–210.
2. Engel A, Fujiyoshi Y, Gonen T, Walz T. Junction-forming aquaporins. *Curr Opin Struct Biol*. 2008;18:229–235.
3. Fotiadis D, Hasler L, Müller DL, Stahlberg H, Kistler J, Engel A. Surface tongue-groove contours on lens MIP facilitate cell-to-cell adherence. *J Mol Biol*. 2000;300:779–789.
4. Kumari S, Varadaraj K. Intact AQP0 performs cell-to-cell adhesion. *Biochem Biophys Res Commun*. 2009;390:1034–1039.
5. Petrova RS, Schey KL, Donaldson PJ, Grey AC. Spatial distributions of AQP5 and AQP0 in embryonic and postnatal mouse lens development. *Exp Eye Res*. 2015;132:124–135.
6. Girsch SJ, Peracchia C. Calmodulin interacts with a C-terminus peptide from the lens membrane protein MIP26. *Cur Eye Res*. 1991;10:839–849.
7. Lindsey Rose KM, Gourdie RG, Prescott AR, Quinlan RA, Crouch RK, Schey KL. The C terminus of lens aquaporin 0 interacts with the cytoskeletal proteins filensin and CP49. *Invest Ophthalmol Vis Sci*. 2006;47:1562–1570.
8. Fan J, Donovan AK, Ledee DR, Zelenka PS, Fariss RN, Chepelinsky AB. GammaE-crystallin recruitment to the plasma membrane by specific interaction between lens MIP/aquaporin-O and gammaE-crystallin. *Invest Opthalmol Vis Sci*. 2004;45:863–871.
9. Fan J, Fariss RN, Purkiss AG, et al. Specific interation between lens MIP/aquaporin-0 and two members of the g-crystallin family. *Mol Vis*. 2005;11:76–87.
10. Mathias RT, Kistler J, Donaldson P. The lens circulation. *J Membr Biol*. 2007;216:1–16.
11. Gerido DA, White TW. Connexin disorders of the ear, skin, and lens. *Biochim Biophys Acta*. 2004;1662:159–170.
12. Gong X, Cheng C, Xia CH. Connexins in lens development and cataractogenesis. *J Memb Biol* 2007;218:9–12.
13. White TW, Goodenough DA, Paul DL. Targeted ablation of connexin50 in mice results in microphthalmia and zonular pulverulent cataracts. *J Cell Biol*. 1998;143:815–825.
14. Rong P, Wang X, Niesman I, et al. Disruption of *Gja8* (a8 connexin) in mice leads to microphthalmia associated with retardation of lens growth and lens fiber maturation. *Development*. 2002;129:167–174.
15. Yu XS, Jiang JX. Interaction of major intrinsic protein (aquaporin-0) with fiber connexins in lens development. *J Cell Sci*. 2004;117:871–880.
16. Liu J, Xu J, Gu S, Nicholson BJ, Jiang JX. Aquaporin 0 enhances gap junction coupling via its cell adhesion function and interaction with connexin 50. *J Cell Sci*. 2011;124:198–206.
17. Yu XS, Yin X, Lafer EM, Jiang JX. Developmental regulation of the direct interaction between the intracellular loop of connexin 45.6 and the C-terminus of major intrinsic protein (aquaporin-0). *J Biol Chem*. 2005;280:22081–22090.
18. Hu Z, Shi W, Riquelme MA, et al. Connexin 50 functions as an adhesive molecule and promotes lens cell differentiation. *Sci Rep*. 2017;7:5298.
19. Shiels A, Bassnett S, Varadaraj K, et al. Optical dysfunction of the crystalline lens in aquaporin-0-deficient mice. *Physiol Genomics*. 2001;7:179–186.
20. Biswas SK, Lee JE, Brako L, Jiang JX, Lo WK. Gap junctions are selectively associated with interlocking ball-and-sockets but not protrusions in the lens. *Mol Vis*. 2010;16:2328–2341.
21. Biswas SK, Jiang JX, Lo WK. Gap junction remodeling associated with cholesterol redistribution during fiber cell maturation in the adult chicken lens. *Mol Vis*. 2009;15:1492–1508.
22. Fudge DS, McCuaig JV, Van Stralen S, et al. Intermediate filaments regulate tissue size and stiffness in the murine lens. *Invest Ophthalmol Vis Sci*. 2011;52:3860–3867.
23. Gong X, Li E, Klier G, et al. Disruption of a_3 connexin gene leads to proteolysis and cataractogenesis in mice. *Cell*. 1997;91:833–843.
24. Tholozan FM, Quinlan RA. Lens cells: more than meets the eye. *Int J Biochem Cell Biol* 2007;39:1754–1759.
25. Kumari SS, Eswaramoorthy S, Mathias RT, Varadaraj K. Unique and analogous functions of aquaporin 0 for fiber cell architecture and ocular lens transparency. *Biochim Biophys Acta*. 2011;1812:1089–1097.
26. Sindhu KS, Gupta N, Shiels A, et al. Role of Aquaporin 0 in lens biomechanics. *Biochem Biophys Res Commun*. 2015;462:339–345.
27. White TW, Gao Y, Li L, Sellitto C, Srinivas M. Optimal lens epithelial cell proliferation is dependent on the connexin isoform providing gap junctional coupling. *Invest Ophthalmol Vis Sci*. 2007;48:5630–5637.
28. DeRosa AM, Xia C-H, Gong X, White TW. The cataract-inducing S50P mutation in Cx50 dominantly alters the channel gating of wild-type lens connexins. *J Cell Sci*. 2007;120:4107–4116.
29. Wang E, Geng A, Maniar AM, Mui BW, Gong X. Connexin 50 regulates surface ball-and-socket structures and fiber cell organization. *Invest Ophthalmol Vis Sci*. 2016;57:3039–3046.

30. Grey AC, Li L, Jacobs MD, Schey KL, Donaldson PJ. Differentiation-dependent modification and subcellular distribution of aquaporin-0 suggests multiple functional roles in the rat lens. *Differentiation*. 2009;77:70–83.
31. Cheng C, Nowak RB, Gao J, et al. Lens ion homeostasis relies on the assembly and/or stability of large connexin 46 gap junction plaques on the broad sides of differentiating fiber cells. *Am J Physiol Cell Physiol*. 2015;308:C835–C847.
32. Gonen T, Cheng Y, Kistler J, Walz T. Aquaporin-0 membrane junctions form upon proteolytic cleavage. *J Mol Biol*. 2004; 342:1337–1345.
33. Gonen T, Sllz P, Kistler J, Cheng Y, Walz T. Aquaporin-0 membrane junctions reveal the structure of a closed water pore. *Nature*. 2004;429:193–197.
34. Konig N, Zampighi GA. Purification of bovine lens cell-to-cell channels composed of connexin44 and connexin50. *J Cell Sci*. 1995;108:3091–3098.
35. Kistler J, Kirkland B, Bullivant S. Identification of a 70,000-D protein in lens membrane junctional domains. *J Cell Biol*. 1985;101:28–35.
36. Gruijters WT. A non-connexon protein (MIP) is involved in eye lens gap-junction formation. *J Cell Sci*. 1989;93:509–513.
37. Zampighi GA, Simon SA, Hall JE. The specialized junctions of the lens. *Int Rev Cytol*. 1992;136:185–225.
38. Dunia I, Recouvreur M, Nicolas P, Kumar N, Bloemendahl H, Benedetti EL. Assembly of connexins and MP26 in lens fiber plasma membranes studied by SDS-fracture immunolabeling. *J Cell Sci*. 1998;111:2109–2120.
39. Slavi N, Rubinos C, Li L, et al. Connexin 46 (cx46) gap junctions provide a pathway for the delivery of glutathione to the lens nucleus. *J Biol Chem*. 2014;289:32694–32702.
40. Baldo G, Gong X, Martinez-Wittinghan FJ, Kumar N, Gilula NB, Mathias RT. Gap junctional coupling in lenses from α_8 connexin knockout mice. *J Gen Physiol*. 2001;118:447–456.
41. Martinez-Wittinghan FJ, Sellitto C, Li L, et al. Dominant cataracts result from incongruous mixing of wild-type lens connexins. *J Cell Biol*. 2003;161:969–978.
42. Martinez-Wittinghan FJ, Sellitto C, White TW, Mathias RT, Paul D, Goodenough DA. Lens gap junctional coupling is modulated by connexin identify and the locus of gene expression. *Invest Ophthalmol Vis Sci*. 2004;45:3629–3637.
43. Sellitto C, Li L, White TW. Connexin50 is essential for normal postnatal lens cell proliferation. *Invest Ophthalmol Vis Sci*. 2004;45:3196–3202.
44. Gu S, Yu XS, Yin X, Jiang JX. Stimulation of lens cell differentiation by gap junction protein connexin 45.6. *Invest Ophthalmol Vis Sci*. 2003;44:2103–2111.
45. Vrensen GF. Early cortical lens opacities: a short overview. *Acta Ophthalmol*. 2009;87:602–610.
46. Heys KR, Truscott RJ. The stiffness of human cataract lenses is a function of both age and the type of cataract. *Exp Eye Res*. 2008;86:701–703.

Investigative Ophthalmology & Visual Science